

Fermi National Accelerator Laboratory

TM-1512

**The Response of a Fermilab-Designed Ion Chamber
in Pulsed Photon Fields**

W. S. Freeman, B. Hartman, F. Krueger, and J. Larson
Fermi National Accelerator Laboratory
P.O. Box 500, Batavia, Illinois 60510

January 26, 1988



Operated by Universities Research Association Inc. under contract with the United States Department of Energy

The Response of a Fermilab-Designed Ion Chamber In Pulsed Photon Fields

by

W. S. Freeman, B. Hartman, F. Krueger, and J. Larson

FERMILAB

January 26, 1988

Introduction

This note reports measurements of the response of a Fermilab-designed area monitor ionization chamber used in Chipmunks and Scarecrows to pulsed photon fields of various intensities and durations. The measurements were made to better define the operating limits of the instruments and to understand the possible effects of recombination and space charge on the dose measured by the instruments in pulsed fields.

Experimental Methods

A pulsed beam from the Argonne National Laboratory 22 MeV electron linac was used to strike a heavy metal (tungsten) target and create an intense beam of brehmstrahlung photons. A cylindrical propane-filled ion chamber used in Chipmunk and Scarecrow detectors (see figure 1a) was placed at beam height at either of two distances (2.04 or 4.57 meters) downstream of the target and with its axis of symmetry oriented perpendicular to the beam direction (see figure 1b). A beam current and pulse width were then selected to give the desired radiation dose to the chamber.

Curves of collected charge versus applied voltage were obtained for several values of dose ranging from 3.76 to 1031 mrad per pulse. Linac pulse widths were either 0.25 or 2.5 μ sec, depending on the required dose. The instantaneous dose rates ranged from about 1.5×10^4 to 4.9×10^5 rads per second. A Keithley model 610C integrating electrometer was used to determine the collected charge from the chamber for each linac pulse.

Prior to taking each series of collected charge versus voltage measurements, packets of three thermoluminescent dosimeter chips (Harshaw TLD700) were placed on the beam axis immediately in front of and behind the ion chamber. The packet covers approximated in thickness and construction the wall of the ion chamber under study. The TLDs were exposed to several pulses (typically five) at the selected value of the linac current and pulse width. They were then removed and the measurement of the collected charge versus voltage was begun.

The dose per pulse on the beam axis was determined by averaging the TLD results (front and back) and then dividing by the number of pulses delivered. The effective doses delivered to the ion chamber were derived from the doses measured on axis with the TLD packets by applying a correction factor that accounted for the variation in the radiation field across the face of the

chamber. This variation was measured at 2 meters distance from the target using 49 TLDs placed in a 7 by 7 array spaced 2 inches apart. By extrapolating to 4.57 meters an equivalent distribution at that distance was obtained. Applying these corrections gave effective doses (averaged over the chamber gas volume) that were 83%(93%) of the on-axis value for 2.04 (4.57) meters irradiation distance.

Pulse-to-pulse uniformity was monitored by measuring the electron beam charge striking the target, which was electrically isolated from the beamline and acted as a Faraday cup. Additional monitoring was provided by scaling the output of a standard Chipmunk detector, complete with integrator and digitizer circuits, placed at 76° to the target and operated at its usual voltage of 800 Volts. For two runs (numbers 7 and 14) no TLD results were available, so the dose per pulse for those runs was obtained by normalizing their monitor ion chamber counts to a run having a known dose measured by the TLDs. The dose per pulse in the monitor chamber was sufficiently small so that no corrections for recombination in it were necessary.

Results

All the data, plotted as the collected charge per unit dose versus the applied voltage, are shown in figure 2. Each data set is for a different value of the dose per linac pulse delivered to the chamber. The uppermost set corresponds to a delivered dose of 3.76 mrad per pulse while the lowest set is for 1031 mrad per pulse. Figure 3 shows a subset of the same data plotted as a function of the dose per pulse for several fixed operating voltages.

The lowest dose run in figure 2 displays good saturation behavior. The charge collected at the standard operating voltage of 800 volts is about 97.5 % of the charge collected at the highest voltage (1800 volts). Figure 3 illustrates the decline in collected charge per pulse at fixed voltage as the ionization per pulse in the chamber increases, and it reveals a considerable lack of complete charge collection even at the highest voltages for the higher dose runs.

Analysis and Discussion

General recombination has been discussed extensively in the literature and will be briefly reviewed here. We follow the discussion of Boag¹. For the present measurements, the linac pulse widths (0.25 and 2.5 μ sec) were small compared to the ion collection times in the chamber (milliseconds) while the time between linac pulses was long compared to the collection time. In this limit it can be assumed that the ionization is produced instantaneously and then completed cleared prior to the next pulse. Thus the significant quantity is the total charge density, ρ , liberated by the pulse rather than the instantaneous dose rate. The positive and negative charge clouds, once created, begin to drift past each other toward their respective electrodes under the influence of the applied electric field. In their region of overlap

recombination can occur. The recombination rate depends on the charge density and overlap volume. There is a universal expression describing the collection efficiency, ϵ , in parallel plate ion chambers which is

$$\epsilon = u^{-1} \ln(1+u), \quad (1)$$

where u is related to the applied voltage, V , the electrode spacing, d , the initial charge density, ρ , and parameters of the fill gas, μ (recombination coefficients and mobilities) through the relation

$$u = \mu \rho d^2 V^{-1}, \quad (2)$$

The gas constant μ is best determined experimentally and will be considered a free parameter in the following discussion.

The same expressions apply for cylindrical chambers provided that the electrode spacing, d , is modified to be the effective gap, d_{eff} . For the present chamber

$$d_{\text{eff}} = 1.04 (r_{\text{outer}} - r_{\text{inner}}) = 3.302 \text{ cm}. \quad (3)$$

The expression for the charge collected per unit dose, Q , as a function of the initial charge density and the applied voltage can be written as

$$Q = Q_0 u^{-1} \ln(1+u), \text{ with} \quad (4)$$

$$u = \kappa (\rho / \rho_0) V^{-1} \quad (5)$$

which is a function of two parameters (Q_0 and κ).

To determine the two constants Q_0 and κ , the data for the lowest dose-per-pulse run (3.76 mrad per pulse) was fit to equation (4) using a least-squares method. The fit constants ($Q_0 = 2.684$ nanoCoulombs mrad⁻¹, $\kappa = 204$ Volts) were then used to calculate curves for the other runs. The initial charge density, ρ , for the other runs (in units of the charge density for the lowest dose per pulse run, ρ_0) was assumed to be given by the ratio of the dose for that run to the lowest dose run as determined by the TLD measurements. No corrections for dose rate effects in the TLD material were necessary since TLD700 material is known to have a negligible dependence on dose rate up to values of 10^{10} rads per second², well above the rates in this series of measurements.

The results are shown in figures 4 through 10. Relatively good agreement between theory and experiment was found for the entire series of measurements. The worst agreement was for

the 188 mrad per pulse data set (figure 9) where the theoretical curve overestimates the response by about 16% at the highest voltage and by about 10% at the usual operating voltage of 800 volts.

To verify that the collected charge did not depend on the linac pulse width, two runs with different pulse widths but nearly the same dose per pulse were done. The comparison is shown in figure 11. The two curves are almost indistinguishable even though the pulse widths differed by a factor of ten. This result verified that the experimental parameters were those of the "pulsed beam" rather than the "continuous beam" case for which a different recombination behavior is expected¹.

Figure 12 displays the collection efficiency as a function of the dose per linac pulse for the 800 volt operating point of the chamber. The solid squares are measurements. The solid curve shows the theoretical dependence for a cylindrical chamber using the fit parameters described earlier. The theoretical curve has been extended to dose values below those actually measured to illustrate the onset of complete charge collection (saturation). The agreement is strikingly good, indicating that the chamber's recombination behavior is close to that expected for an ideal cylindrical ion chamber.

This curve can be used to estimate the collection efficiency of a Chipmunk or Scarecrow when exposed to a pulsed field of known dose or dose-equivalent. As a typical example consider the hypothetical "one-pulse accident" where a full intensity beam pulse is lost in a localized region of the accelerator or beam line. If the loss occurs on a time scale of a few microseconds then the conditions are similar to those encountered in the tests reported here and these results can be applied. (This assumes that no differences in recombination occur due to the incident radiation being neutrons rather than photons.) If the true dose per pulse is 100 mrad then the collection efficiency is about 30%. With a Chipmunk quality factor of five(5), this means that a 500 mrem per pulse dose-equivalent is also underestimated by about a factor of three. Pulsed field collection efficiencies accurate to about 10% (relative error) can also be calculated from the following expression:

$$\epsilon = 14.745 \delta^{-1} \ln(1+.06782 \delta) \quad (6)$$

where δ is the dose expressed in mrads per pulse. The second column of Table 1 shows some values calculated using this formula. It should be recalled that this discussion applies only to fields with pulse widths small compared to the chamber ion collection time.

In addition, there is a systematic uncertainty in the delivered dose-per-pulse that is common to all the data (see Appendix). This uncertainty means that the true dose-per-pulse for all data sets could be larger than the TLD-based values by as much as a factor of two. The uncertainty comes from measured differences in the recorded dose that depends on the type of

dosimetry used (e.g. TLD, film badge, pocket ion chamber). A consequence of this uncertainty is that the dose scale on the horizontal axis of figure 12 could be multiplied by a constant that is as large as a factor of two. Strictly speaking, the efficiencies derived from equation (6) or figure 12 should be considered lower limits on the true efficiency. This is a conservative choice from a safety standpoint since the use of an efficiency that is *less than* the true value will result in a correction that *overestimates* the dose. The third column of Table 1 illustrates the effect on the efficiency if the true dose-per-pulse in the measurements was two times the TLD-based dose.

Conclusions

A standard one-atmosphere propane-filled ionization chamber used in Fermilab Chipmunk and Scarecrow area monitors was tested in pulsed gamma-ray fields up to dose rates somewhat greater than 1000 mrad per pulse and for pulse widths shorter than the characteristic ion collection time. The chamber behaved as expected based on a comparison with simple theory. Good relative agreement with the expected theoretical dependence of efficiency versus dose was obtained at the standard operating voltage over a wide range of dose per pulse. A simple parameterization of the efficiency as a function of the dose per pulse was derived.

Acknowledgements

The helpful comments of Alex Elwyn are gratefully acknowledged, as is the help of Chuck Salsbury in TLD processing. Thanks also to the ANL electron linac staff for operation of the accelerator.

REFERENCES

1. Attix, et. al., Radiation Dosimetry, volume II, Academic Press, Chapter 9, pages 11-27 (1966).
2. Cameron, J.R. et.al., Thermoluminescent Dosimetry, Univ of Wisconsin Press, pages 32-34 (1968).

APPENDIX

Analysis of Fill Gas Parameter

The value of κ (204 volts) found from the fit to equation 4 can be used to determine the parameter μ for the propane gas filling the chamber. Recall that

$$\kappa = \mu d_{\text{eff}}^2 \rho_0$$

where ρ_0 is the initial charge density for the lowest dose data set. Taking ρ_0 equal to 4.5×10^{-3} nC-cm⁻³ as determined from the the measured value of the chamber plateau curve in figure 4, the value of μ is found to be 1390 V-cm-esu⁻¹. According to Boag¹, values for an air-filled chamber range from 1000 to 1250 V-cm-esu⁻¹ at 760 mm Hg and 20^o C based on calculations using published values of the recombination coefficient and ion mobilities. An experimental value of 1090 V-cm-esu⁻¹ for an air-filled chamber has also been reported¹. Since

$$\mu = \alpha / (k_+ + k_-)$$

these results imply that the recombination coefficient, α , for propane is slightly larger than the one for air and/or the mobilities (k_+ , k_-) are slightly smaller for the same gas temperature and pressure.

Analysis of Chamber Sensitivity and Dosimetry

The fit constant Q_0 (2.684 nC-mrad⁻¹) is a measure of the chamber sensitivity. Its numerical value is determined by the dose per pulse delivered to the chamber. This value can be compared to the sensitivity as determined by exposure of the chamber to a calibrated beam of ¹³⁷Cs photons under low dose rate conditions (~100 mR/hr) in order to obtain an estimate of the systematic uncertainty in the dose measurements for the pulsed beam tests. The ¹³⁷Cs calibration value of the sensitivity is 1.84 nC mrad⁻¹. Thus, the pulsed-beam data based on TLD dosimetry shows a *higher* sensitivity by about a factor of 1.46.

The value of Q_0 stated above was derived using TLD chips whose calibration factors were obtained from exposures to ¹³⁷Cs gamma rays. In addition to TLDs, three types of commercial dosimeters (Landauer P1, B1 and H1 film badges) were included in the pulse tests, as were Dosimeter Corporation pocket ion chambers. All dosimeter types were simultaneously mounted on the front and back of the Chipmunk chamber and subjected to a variety of exposures. A comparison of the results (front and back average values) is shown in figure 13. The film badges systematically indicated a higher dose per pulse than the TLDs, while the pocket ion chambers were in reasonable agreement with the TLD doses. The different types of Landauer badges show a variation by as much as 35% among themselves, even though the beta-gamma film

portion of the dosimeters is nominally identical. If the B1 badge doses were used to normalize the collected charge per pulse data rather than the TLD doses, then the pulsed-beam sensitivity would be 73 % of the value found with the ^{137}Cs calibration beam, leading to the conclusion that the chambers are slightly *less* sensitive in the higher energy pulsed photon field environment of the Linac than in the 662 keV field of the ^{137}Cs source.

A calculation (based on NCRP 51) of the expected photon dose rate at zero degrees from a 20 MeV electron beam striking a high-Z target gave results in good agreement with the TLD700 doses. A similar calculation of the expected dose rate from neutrons showed them to be a negligible component. This was consistent with the minimal neutron doses recorded by Landauer badges. Thus the apparent increase in sensitivity (based on TLD doses) for the Linac measurements cannot be explained by a significant neutron component in the radiation field to which the ion chamber is sensitive but the TLD700 is not.

In the absence of a preferred choice of dosimetry to fix the "true" dose scale, the full spread in the dosimetry results can be taken as an indication of the overall systematic uncertainty in the dose per pulse. This leads to the conclusion that the dose per pulse scale (see figure 12, for example) is correct only to within a factor of two, with the TLD-based doses being considered a lower limit on the dose per pulse and the B1 film badge results an upper limit. If the sensitivity obtained from the ^{137}Cs calibration is taken to be the "correct" value, then the systematic error between it and the dose per pulse inferred from the TLDs is somewhat smaller, about 46%. Note that none of the discussion in this section affects the other conclusions in the the paper since all those results were dependent on the dose per pulse expressed as a *ratio* to the lowest dose-per-pulse data set.

Table 1

Ion chamber charge collection efficiencies for several values of the dose per pulse.

True Dose per Pulse (mrad)	Efficiency	
	(a)	(b)
0.1	1.0	1.0
1.0	.97	.98
10	.76	.86
100	.30	.44
1000	.06	.10

(a) based on dose-per-pulse derived from TLDs

(b) based on dose-per-pulse that is two times TLD dose

Figure Captions

1. a) Illustration of cylindrical ion chamber design.
 b) Experimental arrangement.

2. Collected charge per unit dose as a function of the voltage applied to the ion chamber for several values of the linac dose-per-pulse. Numbers adjacent to each of the data set symbols in the legend denote the dose-per-pulse (in mrad) for that data.

3. Collected charge per unit dose as a function of the dose-per-pulse for several values of the voltage applied to the chamber.

- 4-10. Comparisons of measured data with calculations based on the theoretical expression of Boag as discussed in the text. The open squares are the measured values; the solid lines are theoretical curves. The dose per pulse for each data set is listed in the title on each figure. The theoretical curve in figure 4 was derived from a least squares fit to the data. All theoretical curves in figures 5 through 10 use the parameters found from the fit of figure 4 as discussed in the text.

11. A comparison of two sets of measurements for different linac beam pulse widths but similar doses per pulse.

12. Measured collection efficiencies of the ion chamber (squares), compared to theoretical curve calculated with fit parameters derived from figure 4 data.

13. A comparison of various dosimetry results, expressed as a ratio to the doses per pulse determined with TLD700 chips. Open (filled) squares are for B1 (P1) badges. Open (filled) triangles are for H1 badges (pocket ion chambers), respectively.

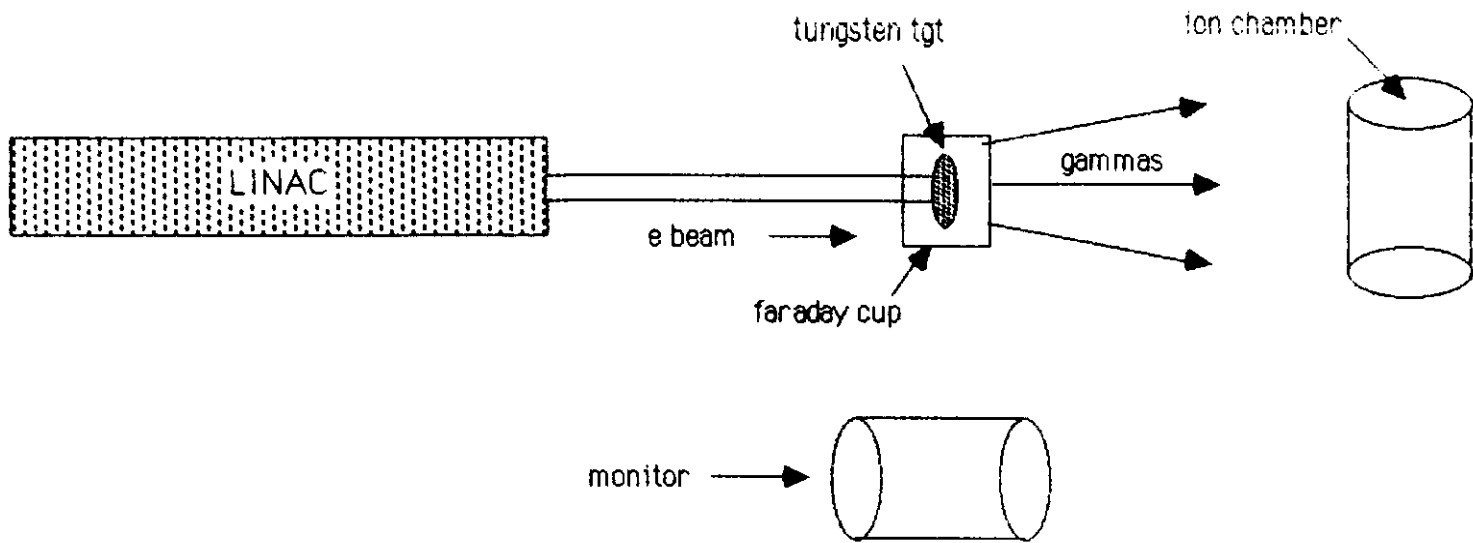


Figure 1B

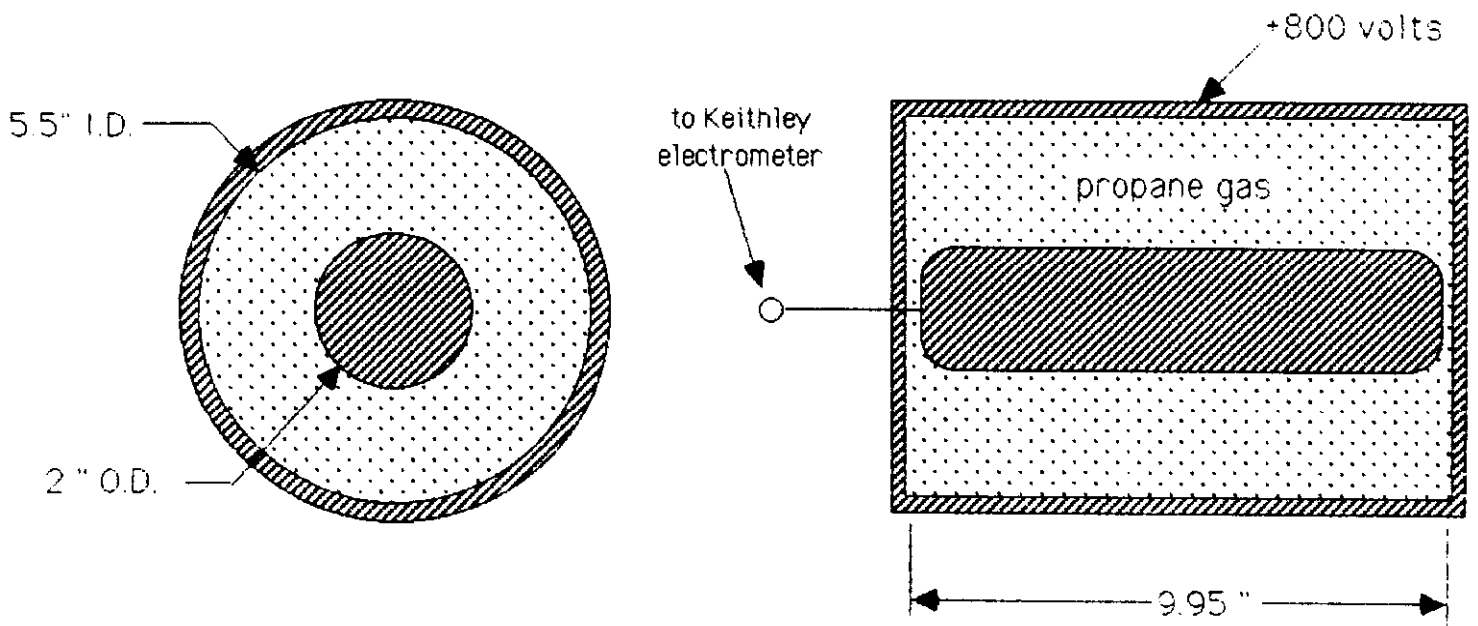


Figure 1A

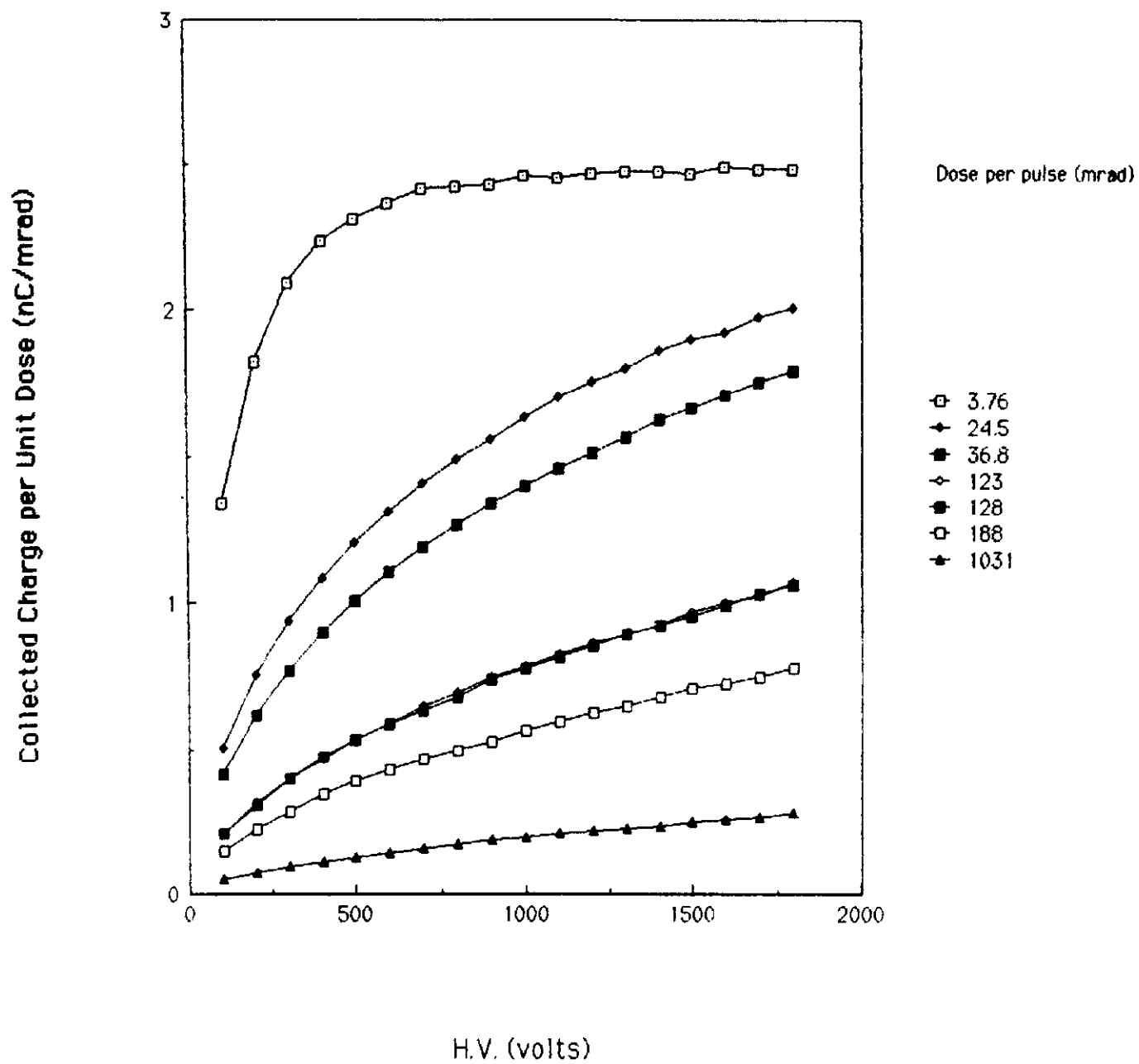


Figure 2

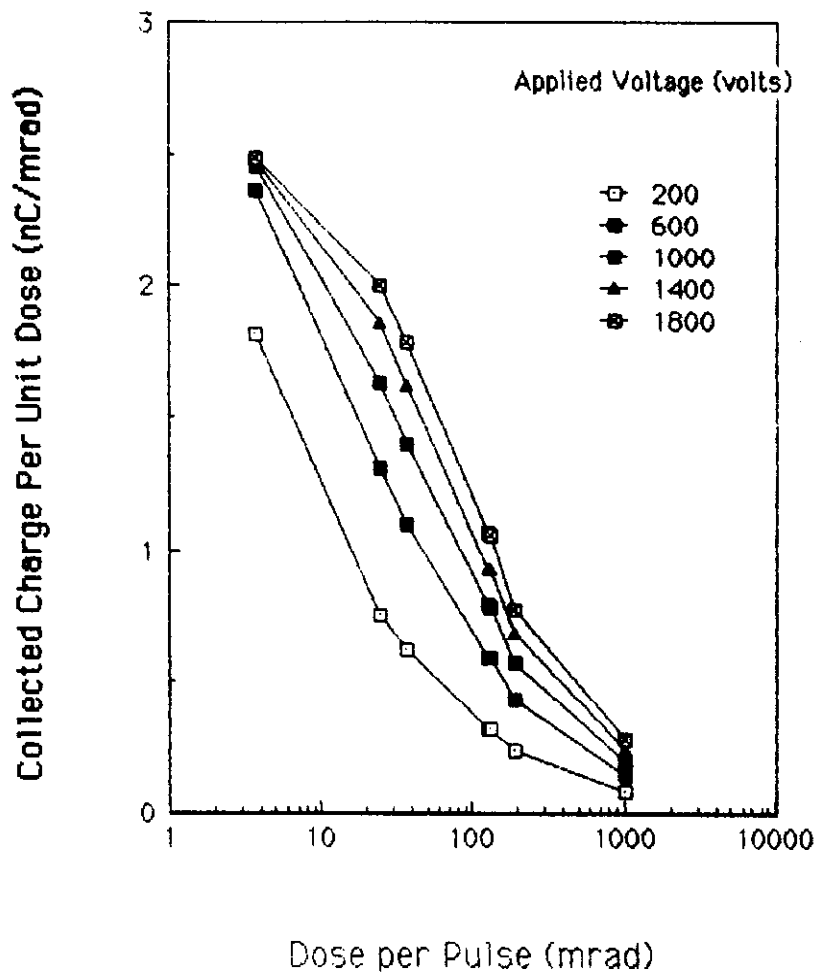


Figure 3

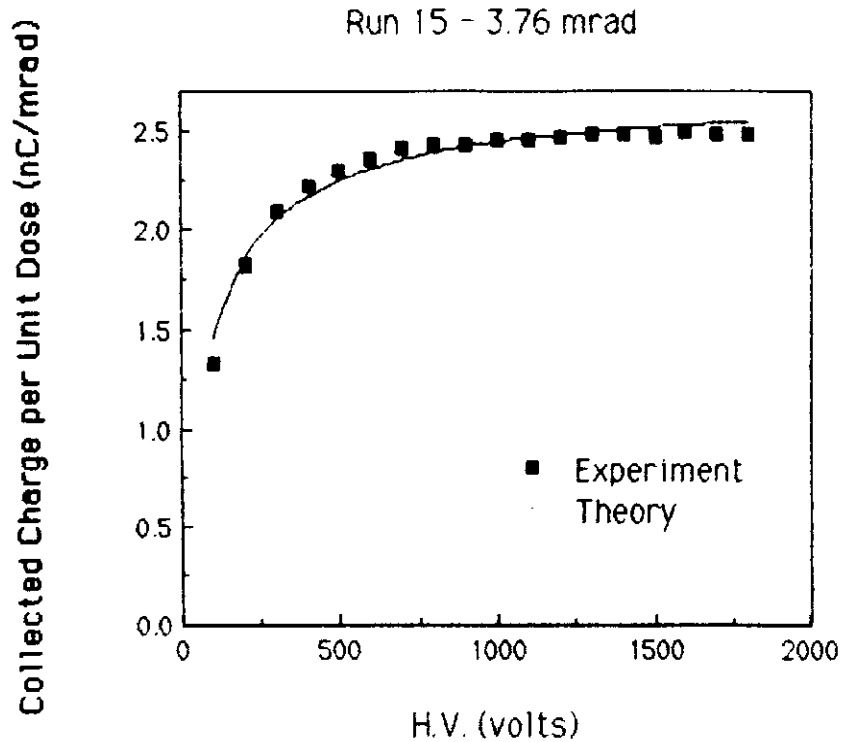


Figure 4

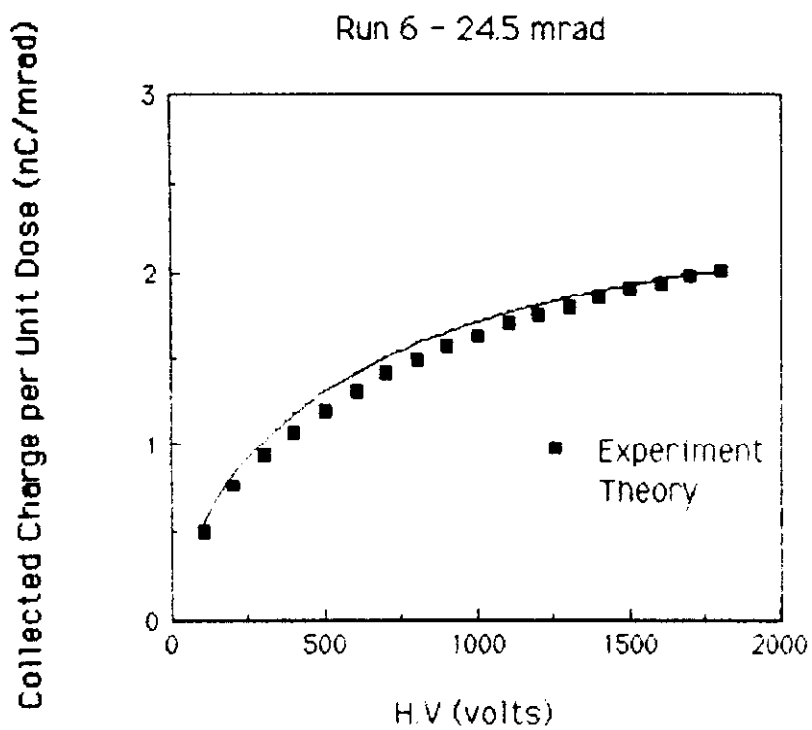


Figure 5

Collected Charge per Unit Dose (nC/mrad)

Run 3 - 36.8 mrad

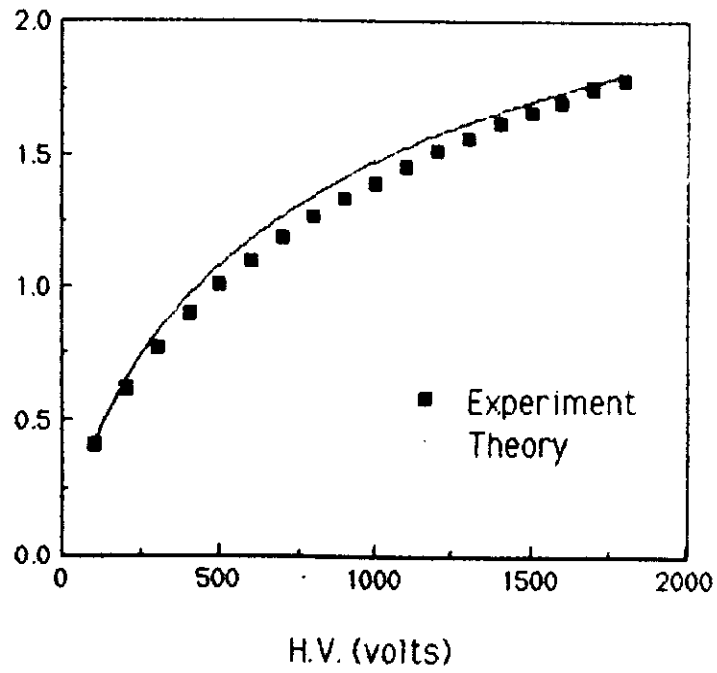


Figure 6

Collected Charge per Unit Dose (nC/mrad)

Run 13 - 123 mrad

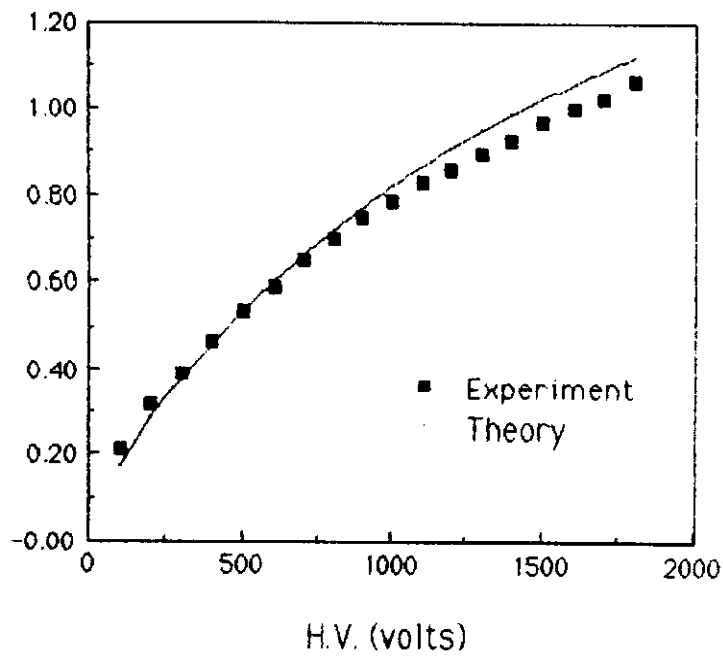


Figure 7

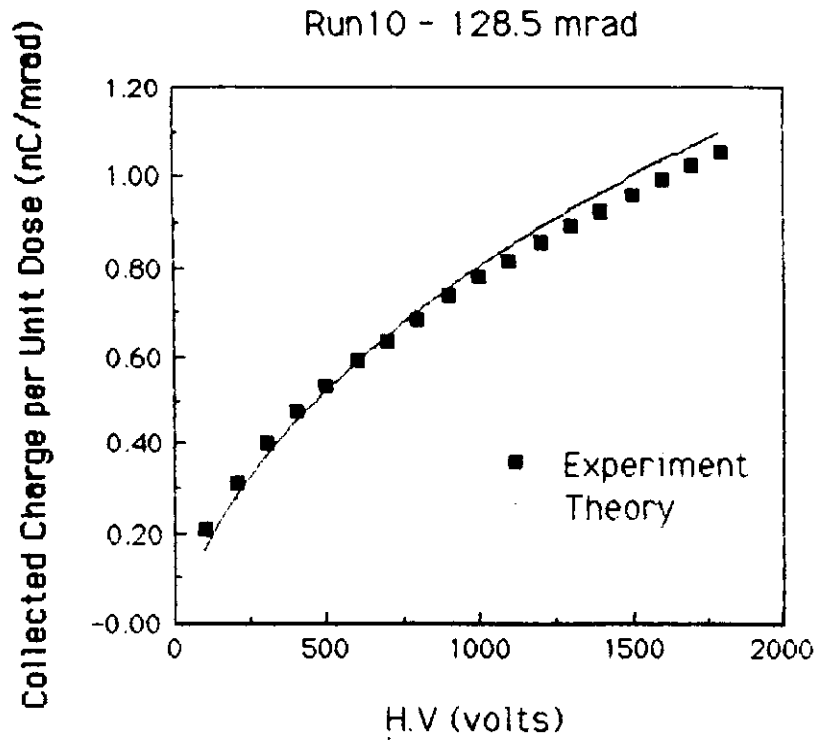


Figure 8

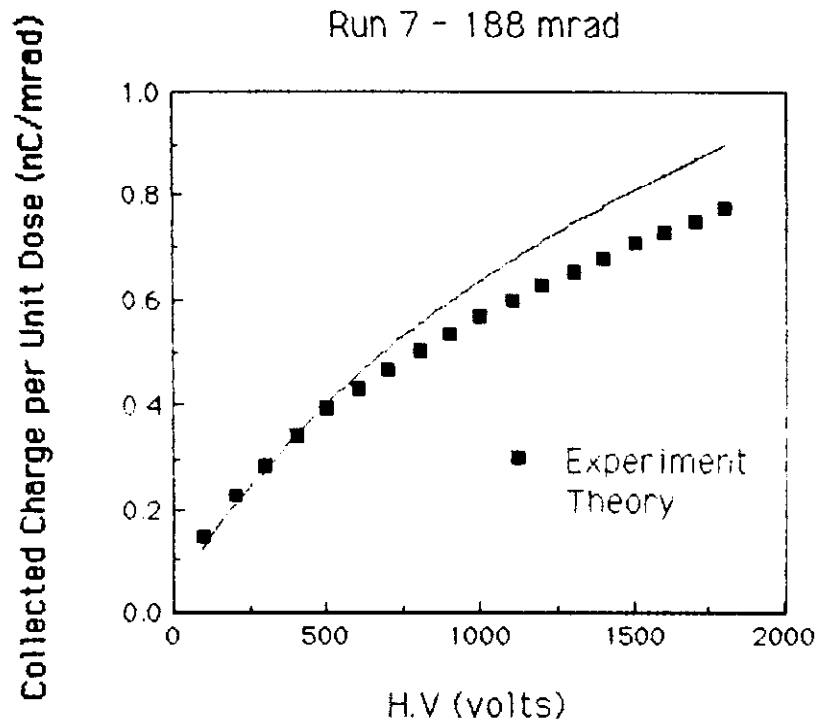


Figure 9

Run 14 - 1031 mrad

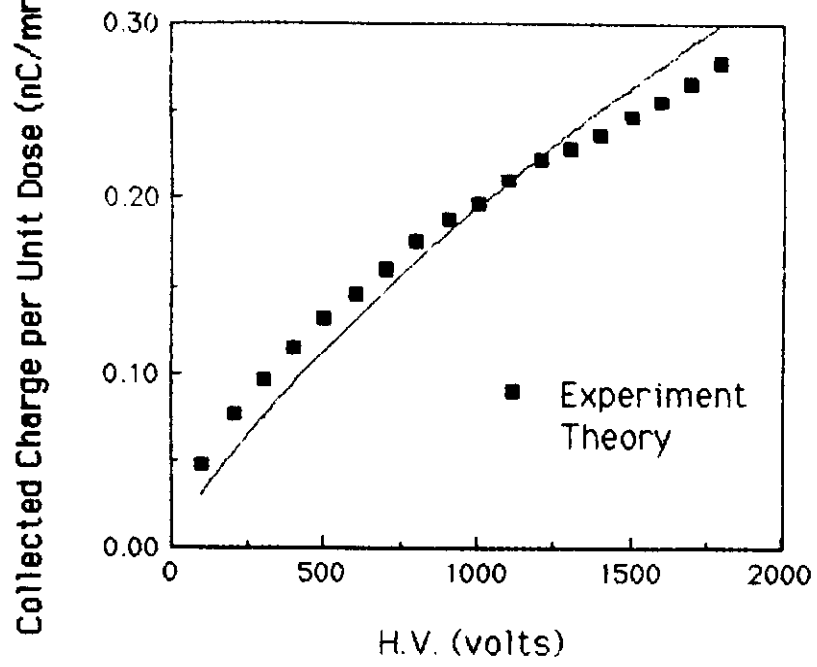


Figure 10

Comparison for Two Linac Pulse Widths

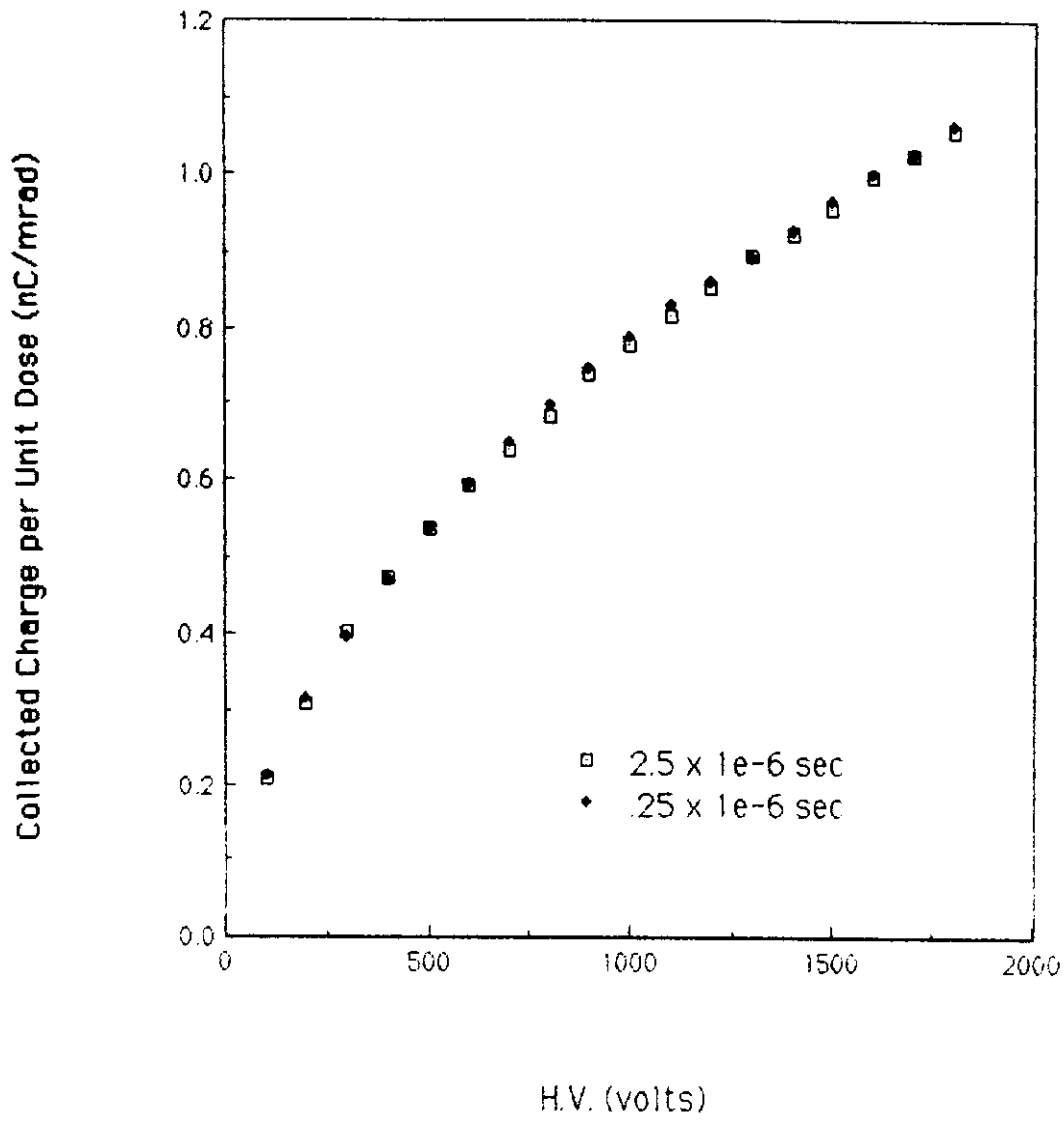


Figure 11

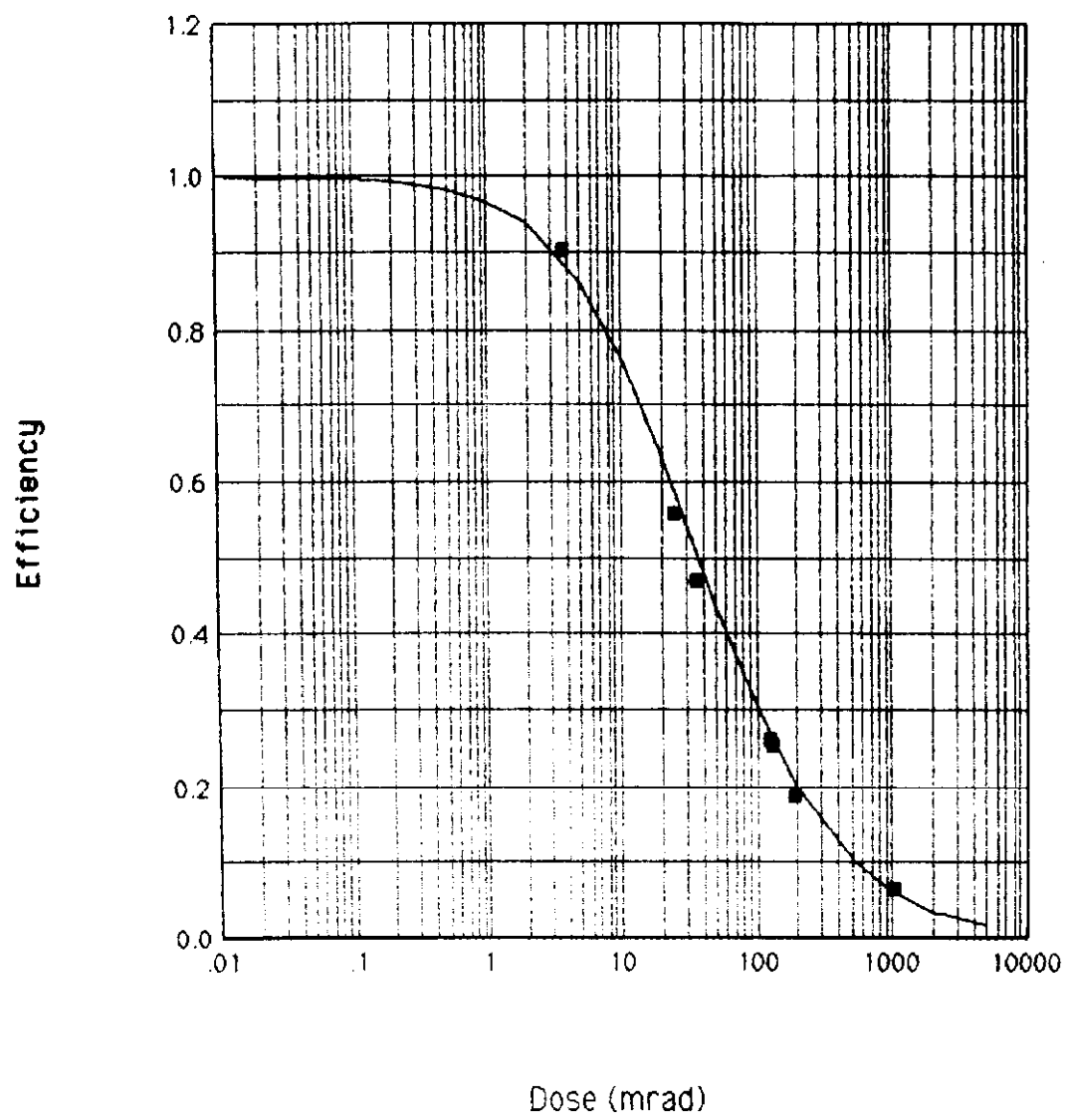


Figure 12

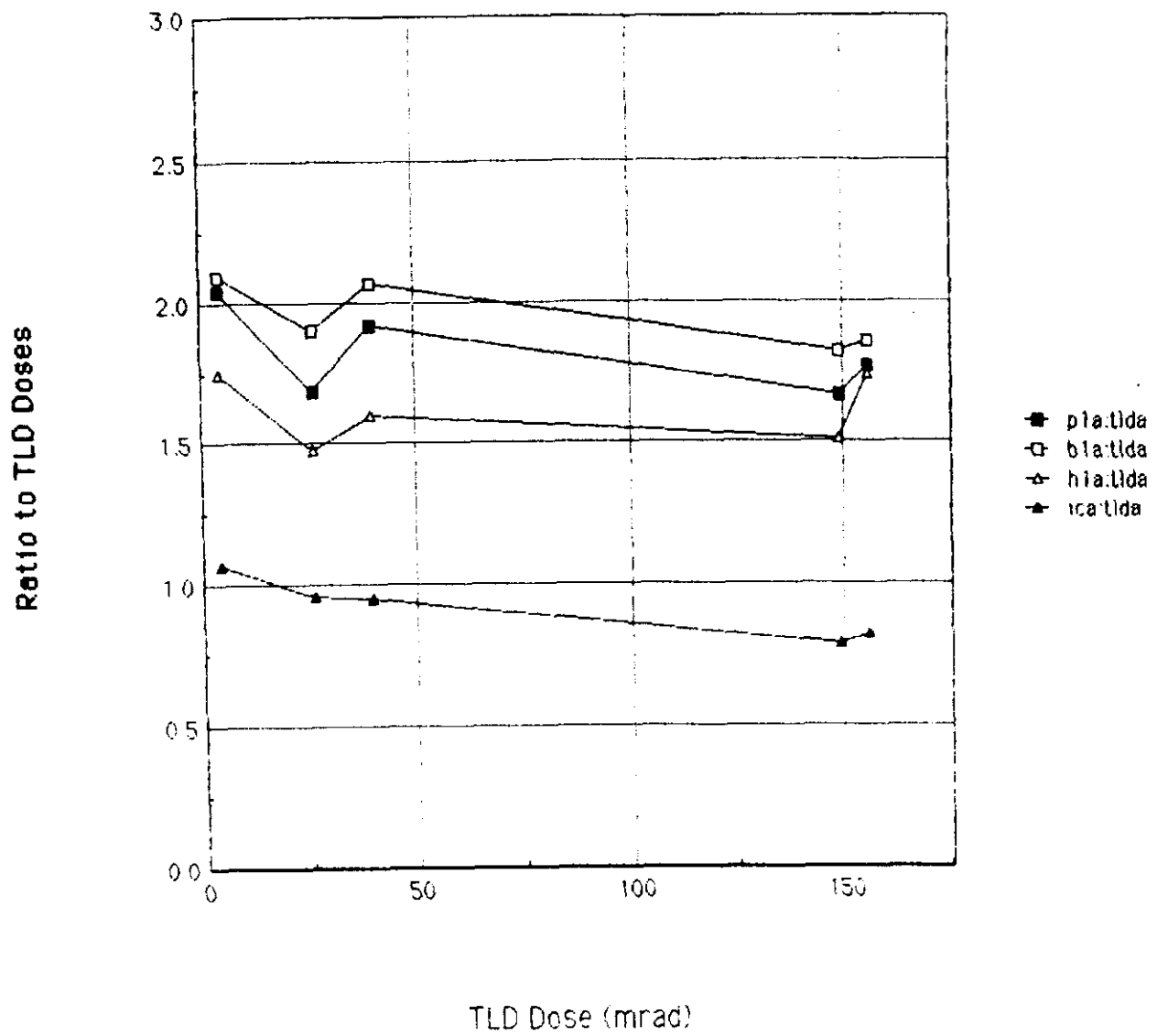


Figure 13